been experimentally confirmed for the first time. However, many problems (for example, concerning the regimes of stabilization and ionization in a strong field) need experimental elucidation. As for the theory of interference stabilization, none of the models available and none of the approaches used are rigorous. Therefore, it is appropriate to continue extensive studies by different methods by comparing the results and finding the most reliable of them. It is also worthwhile extending the regions of parameters of exact numerical solutions and experimental studies. One of the most important new theoretical results is the possibility of stabilization of atoms in the case of long pulses ($\tau \gg t_K$) by increasing the field intensity. This result was obtained using a model of equations for the probability amplitudes $C_n(t)$ and has not yet been confirmed by other methods. In this connection, it is very important to extend the region of applicability of the solution based on the quasi-classical approach to pulses of long duration. It is also important to extend the range of parameters in which the problem can be exactly solved numerically.

References

1. Gavrila M, Kaminski J Z *Phys. Rev. Lett.* **52** 613 (1984)
2. Fedorov M V, Movsesian A M *J. Phys. B* **21** L155 (1988)
3. Hoogenraad J H, Vrijen R B, Noordam L D *Phys. Rev. A* **50** 4133 (1994)
4. De Boer M P et al. *Phys. Rev. A* **50** 4085 (1994); Van Druten N J et al. *Phys. Rev. A* **55** 622 (1997)
5. Gavrila M, in *Atoms in Intense Laser Field*s (Ed. M Gavrila) (Boston: Academic Press, 1992) p. 435
6. Kulander K C *Phys. Rev. A* **35** 445 (1987)
7. Kulander K C et al. *Phys. Rev. Lett.* **66** 2601 (1991)
8. Javanainen J, Eberly J H, Su Q *Phys. Rev. A* **38** 3430 (1988)
9. Fedorov M V *Atomic and Free Electrons in a Strong Light Field* (Singapore, River Edge, NJ: World Scientific, 1997)
10. Fedorov M V *Laser Phys.* **3** 219 (1993)
11. Fedorov M V *J. Phys. B* **27** 4145 (1994)
12. Fedorov M V et al. *J. Phys. B* **29** 2907 (1996)
13. Woiczik A, Parzynski R *Laser Phys.* **7** 551 (1997)
14. Tikhonova O V, Fedorov M V *Laser Phys.* **7** 574 (1997); *Acta Phys. Pol.* **93** 77 (1998)
15. Fedorov M V, Tikhonova O V *Phys. Rev. A* **58** 1322 (1998)
16. Fedorov M V, Fedorov S M *Opt. Express* **3** 271 (1998)
17. Tikhonova O V et al. *Laser Phys.* **8** 85 (1998)

PACS number: 42.55.Vc

Hard X-ray radiation and fast particle generation using multiterawatt laser pulses

A A Andreev, A V Charukhchev, V E Yashin

1. Introduction

It is known that a laser plasma is an intense source of X-ray radiation and fast particles. This problem has been studied for nanosecond plasma in many papers [1]. At present, due to the advent of powerful picosecond and subpicosecond lasers, the possibility of generating X-rays and fast particles produced upon interaction of radiation from these lasers with solid targets in vacuum has appeared (see, for example, Ref. [2]). The physics of the interaction of ultrashort ($\tau \leqslant 1$ ps) powerful ($I > 10^{15}$ W cm^{-2}) laser pulses with solid targets considerably differs from the situation with long (nanosecond) pulses, because in this case the target material practically does not disperse, resulting in the formation of a high-temperature dense plasma in a small volume. This plasma is an intense source of X-ray radiation with the energy of quanta achieving several tens of MeV, and also of fast particles, first of all electrons, ions, positrons, and even muons [3].

In this article, we consider questions related to the generation of X-ray radiation and fast particles produced upon irradiation of solid targets by picosecond laser pulses with intensities exceeding 10^{16} W cm^{-2}. We will mainly analyze the results of experiments performed on our laser setups using such laser intensities.

2. Laser systems

To produce high intensities of focused laser radiation, we used two Nd:glass laser systems with the amplification and compression of a chirped pulse [4]. The laser system developed in the Institute of Laser Physics (Fig. 1) produced 1.5-ps pulses with an energy of up to 2.5 J and almost diffractive angular divergence of radiation. These pulses provided the intensity of radiation focused onto a spot of diameter about 10 μm up to 10^{18} W cm^{-2}. The high contrast of the pulse power, up to 10^7, was provided by a system of Pockels cells and electro-optical deflectors. Note that in a number of plasma experiments related, for example, to the optimization of the integrated yield of X-ray radiation, it is necessary to generate not only a single ultrashort pulse but also a train of pulses with a controllable time interval between them. Such a pulse train with the time interval controlled within 5 – 200 ps was obtained in this laser system by time multiplexing of the ultrashort pulse train from a master oscillator (MO) in a regenerative amplifier (RA) [5]. In this case, the pulse-repetition period was determined by the difference in bases of the resonators of the MO and RA, and the relative amplitude of a pulse in the train is controlled by electro-optical elements.

The laser system developed in the Institute of Complex Testing of Optical and Electronical Systems [6] differs from the above system by the method of obtaining a chirped pulse and the sizes of output amplifier cascades and diffraction gratings of the compressor. The high contrast of the laser pulse was provided by a multicascade electro-optical system based on Pockels cells. A block diagram of this system is presented in Fig. 2. It consists of four main parts: a driving laser system [6], a powerful amplifier cascade based on a 'Progress' amplifying channel [7], a compressor with holographic gratings, and a focusing system [8].

The driving laser produces chirped pulses of duration of the order of 300 ps and an energy of up to 1 J at a wavelength of 1053 nm. These pulses are then amplified in a powerful amplifier or compressed to 1.5 ps with the help of two 1700 lines mm^{-1}, 110×170 mm diffraction holographic gratings to perform plasma experiments with a power density of the order of 10^{17} W cm^{-2}.

A single pulse is separated and gated in a system of four Pockels cells, which are controlled by synchronized high-voltage electric pulse generators based on drift diodes with fast restoration of the reverse voltage [9]. These generators produce electric pulses of 1.5 – 5 ns duration at the half-height with amplitudes up to 15 kV.

The power of laser pulses was increased to 20 – 30 TW in a three-cascade amplifier channel containing three Nd:glass rod amplifiers with apertures 4.5, 6, and 8.5 cm and 30 cm in length [10].

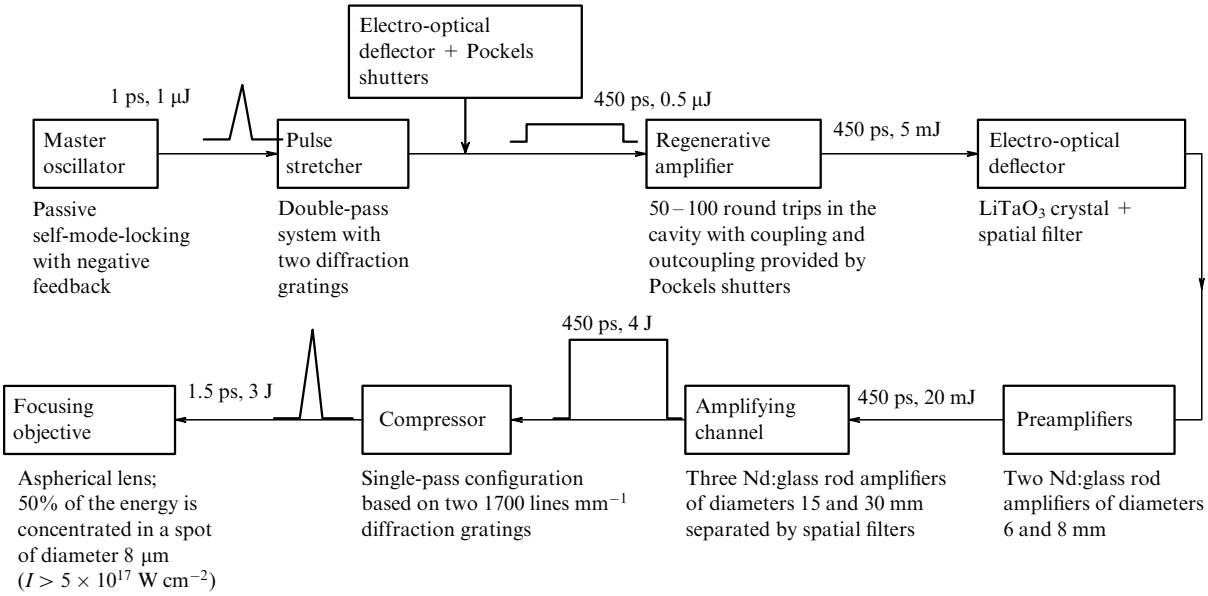

Figure 1. Block diagram of the laser system for pulse generation, amplification, and compression (Institute for Laser Physics).

The 300-ps pulse at the output of the amplifier is compressed in a single-pass compressor consisting of two 1600 lines mm^{-1}, 21 × 42 cm holographic gratings with a gold coating.

The duration and spectral width of the compressed pulse at the entrance to the target chamber are 1.5 ps and 1.5 nm, respectively. The laser beam enters the target chamber through a high-quality vacuum window made of LiF crystal with a small nonlinear addition to the refractive index $n_2 \sim 0.35 \times 10^{-13}$ CGSE units.

The laser beam of diameter 37 mm (the driving system) is focused onto the target by a 13 mm thick aspherical lens with a focal length of 140 mm, which concentrates 75% of the beam energy into the diffraction limited 9.7 μm spot, or by an off-axis parabolic mirror with a focal length of 120 mm, which focuses 65% of the ideal beam energy to a spot of diameter 7.2 μm. In the case of focusing by the lens, the lens itself is the vacuum window. These focusing systems were used in experiments at power densities not exceeding 2×10^{17} W cm^{-2}.

To focus more powerful beams, up to 30 TW, an axial parabolic mirror 200 mm in diameter with an aperture ratio of 1:1 was used, which concentrated 50% of the ideal beam to a 5-μm spot. The resulting average power density of the laser radiation focused on the target achieved $5 \times 10^{18} - 10^{19}$ W cm^{-2}.

The amplified spontaneous emission propagated through the output compressor was measured with a fast diode and calorimeter and did not exceed 10 μJ for 5 ns ahead of the pulse maximum. The energy contrast of the laser pulse was no less than 10^5. The time interval between laser pulses did not exceed 35 min.

The possibility of obtaining of such high radiation intensities was controlled both by optical and X-ray methods and was provided by high-quality optical elements in the laser systems. As an example we present the parameters of diffraction gratings used for the pulse compression in the Table. These parameters provide a certain safety factor and should allow one to increase the radiation intensity at least several times compared to the existing level.

Table. Parameters of diffraction gratings for pulse compression.

Grating type	Number of lines per mm	Metal	Maximum size, mm	Damage threshold W_{th}, mJ cm^{-2} (1 ns/1 ps)
Ruled	1740	Au	170 × 170	360/240
Holographic	1700	Au	210 × 420	320/180
Holographic	1700	Au with coating	210 × 420	560/230

3. Interaction of the intense laser radiation with the matter

The action of the intense laser pulse on a solid target induces various channels of generation of radiation and particles according to the following scheme:

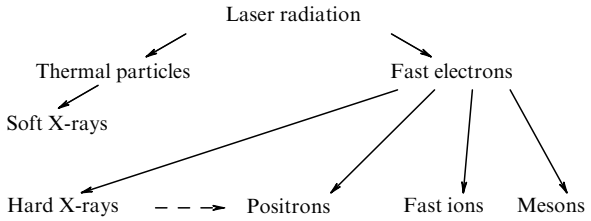

3.1 Absorption of the laser pulse

We start to consider the generation of X-ray radiation from analysis of mechanisms of absorption of laser radiation in a plasma, because they determine the coefficient of transformation of the laser energy to the energy of X-rays and particles.

It is known that for laser intensities $I_L > 10^{15}$ W cm^{-2} the electron temperature increases quite rapidly, so that collision absorption becomes inefficient [14]. In addition, the oscillation velocity v_E of electrons becomes comparable with their thermal velocity, which also reduces the effective frequency of collisions [15]. Therefore, at intensities above 10^{16} W cm^{-2} non-collision mechanisms of relaxation begin. For example, it

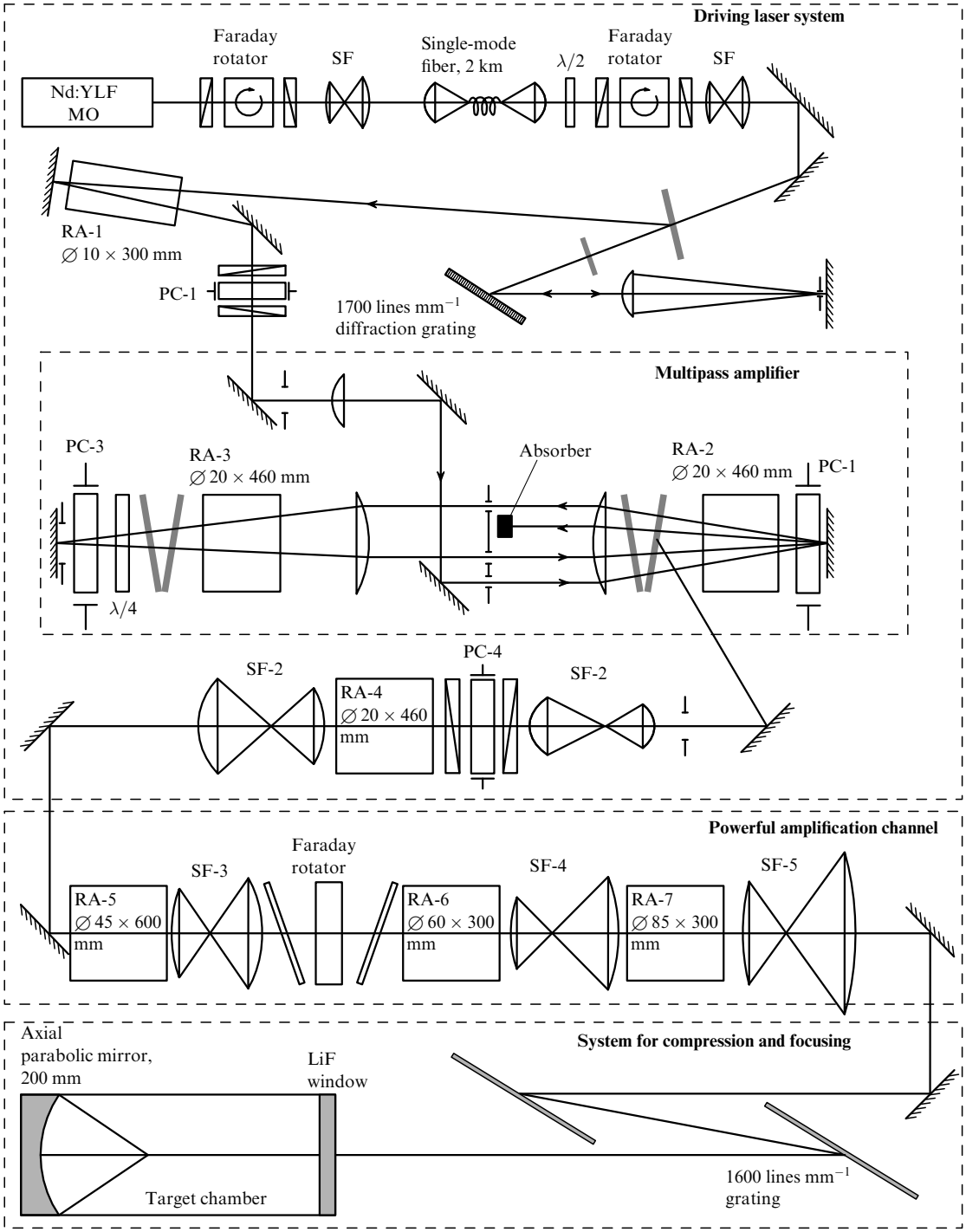

Figure 2. Optical scheme of the 'Progress-P' Nd:glass laser system.

was found that for intensities above 10^{16} W cm^{-2}, the absorption amounts to 50% [11 – 13].

Under the conditions of our first experiments, when the laser radiation intensity was lower than 5×10^{17} W cm^{-2}, resonance absorption played the main role [17, 18]. The results of experiments and calculations of the absorption coefficient as a function of the angle of incidence θ of the laser pulse using the SKIN hydrodynamic code are in agreement with Refs [16, 31]. In the program, we describe the resonance absorption with the help of a model [32] supplemented with the mechanism of nonlinear overturn of the plasma wave [33]. Our description of the transfer of fast electrons deep in the target is analogous to that in Ref [34], however, we made no assumptions about the number and energy of fast electrons but calculated this from laser parameters. The model of acceleration of fast ions is based on the mechanism of acceleration in the ambipolar field [35]. In this case, the absorption coefficient can be approximately written in the form [19]

$$A_{\mathrm{r}} \approx \frac{\sin^2\theta}{\cos\theta} kL\,,$$

here, $k = \omega/c$, and L is the inhomogeneity scale in the vicinity of the critical concentration n_{c}. When the amplitude r_E of the

electron oscillations in the laser-wave field exceeds L, we have Brunel absorption [20]:

$$A_{\mathrm{B}} \approx a\frac{\sin^3\theta}{\cos\theta}kr_E\,.$$

At high temperatures, the absorption coefficient after the pulse termination, in the regime of the anomalous skin effect, has the form [21]

$$A_{\mathrm{a}} \approx \frac{2.8kl_{\mathrm{s}}}{\cos\theta}\,,$$

where $l_{\mathrm{s}} = \max\{L, l_{\mathrm{sa}}\}$.

For subrelativistic intensities, when the difference in absorption of S- and P-polarized waves decreases because of the strong ponderomotive pressure, the absorption coefficient for normal incidence has the form [24]

$$A_{\mathrm{c}} \approx 16\pi\left(\frac{v_E}{c}\right)^2(kL)^3\ln^2\left(\frac{1}{2kL}\right).$$

For ultrarelativistic intensities ($v_E > c$), the laser pulse acts on the plasma as a piston, accelerating the ions [25]. In this case, the absorption coefficient is

$$A_i \approx 3\times10^{-3}\left(\frac{n_{\mathrm{c}}}{n_{\mathrm{e}}}\right)^{1/2}kr_E\,.$$

These approximations were verified by calculations using the one-dimensional KINET kinetic code, which consists of two parts: the first part solves the Boltzmann equation in the region of the laser field and the second solves the Fokker–Planck equation on the mean free path of an electron [61]. We found that the results of calculations agree with scaling and our experiments [59, 60] (Fig. 3). However, in the latter case, there is some difference and the agreement is only qualitative. The important effects that distort the one-dimensional picture are 'deepening' and 'riffling' of the target surface [26] caused by the excess of the light pressure over the plasma pressure: a plasma will move inside the target and absorption will increase. The appearance of a strong magnetic field [22, 23, 27–30] changes the resonance properties of a plasma, and the dependence of the absorption coefficient on θ has no maximum as in the case of low intensities [48].

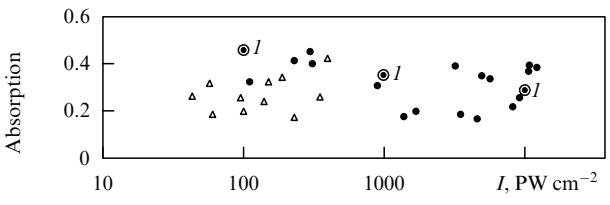

Figure 3. Absorption of P- (•) and S-polarized (△) laser radiation by an aluminium target as a function of the radiation intensity. Points *1* were calculated using the KINET code.

3.2 Transport of electrons in a laser plasma

The depth of heating of the substance by the thermal wave and fast electrons is no less important than absorption for the generation of X-rays. The SKIN calculations showed that this heating provided by fast electrons whose mean free path is $l_{\mathrm{h}} \propto T_{\mathrm{h}}^2/n_{\mathrm{i}}$ for laser radiation intensities of 10^{17} W cm^{-2}. At large radiation intensities, the flux of fast particles is so great that the ambipolar substantially limits it. Because at such intensities the hydrodynamic description is inadequate, we performed a simulation using the KINET code and found that when the electron velocity $v_{\mathrm{he}} \ll c$, the distribution function becomes isotropic over angles in the region of a dense plasma and the electron mean free path is close to l_{h}. If $v_{\mathrm{he}} \approx c$, the term in the collision integral describing the e–e collisions becomes dominant, and the length of heating is $l_{\mathrm{lim}} \approx T_{\mathrm{h}}^2/(n_{\mathrm{i}}/b + e^2A_iI_{\mathrm{L}}/\sigma)$. Note also that in this case the electron current produces a strong magnetic field, which also limits the electron transport [36].

3.3 Intensity of X-ray radiation

Having measured the absorption of laser radiation and the length of heating of the plasma, we calculated the intensity of X-ray radiation for a continuous spectrum and in lines [37]. The intensity and spectrum of X-ray radiation were measured with an eight-channel X-ray analyzer. Irradiation of Al targets by picosecond laser pulses with $I_{\mathrm{L}} < 10^{17}$ W cm^{-2} showed that the coefficient of conversion to relatively soft X-rays was $k_{\mathrm{X}} = 2\,\%$. Calculations with the help of the one-dimensional hydrodynamic ION code [37], in which the charge composition of a plasma was calculated in the kinetic approximation, showed that under our conditions the duration of X-ray radiation was about 20 ps and the conversion coefficient increased with increasing intensity and duration of the laser pulse. Note that conversion of the laser radiation to the Ly–α and He–α lines of the aluminium target proved to be quite high ($\sim 0.5\,\%$), which could be used for the development of a monochromatic, bright X-ray source. In this case, the condition of equality of the mean free paths of the X-ray quantum and the fast electron can be considered optimum ($L_{\mathrm{X}} \approx l_{\mathrm{he}}$). The intensity of X-ray radiation of a laser plasma can be significantly increased by producing a preplasma with the help of a profiled train of picosecond pulses [38]. Calculations performed for a train of picosecond pulses showed (Fig. 4) that the intensity of bremsstrahlung and recombination radiation increases with the distance between pulses, while the intensity of the He–α line (for the aluminium target) has a maximum for a 30-ps delay. Estimates show that the optimum delay time between pulses is $\Delta\tau \propto (L_{\mathrm{Li}}/T_{\mathrm{e0}})^2\tau$, where I_{Li} is the ionization

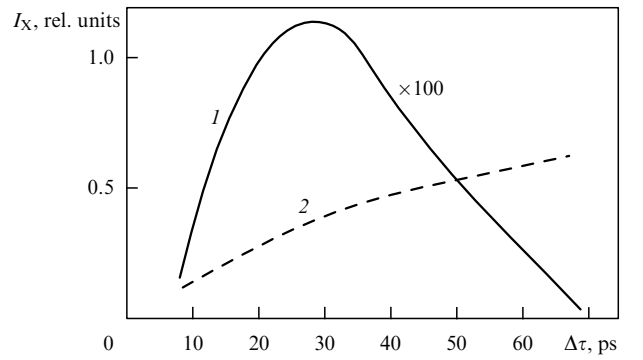

Figure 4. Dependence of the intensity I_{X} of X-rays emitted by a plasma on the time delay $\Delta\tau$ between two pulses for the integrated bremsstrahlung and recombination emission (*1*) and emission in the 1.6-keV He–α line (*2*).

potential of the Li-like ion, T_{e0} is the temperature of plasma produced by a prepulse, and τ is the laser pulse duration.

In contrast to soft X-rays, hard X-rays directly result from generation of fast electrons in the vicinity of the focal spot. Due to their large mean free path, fast electrons can penetrate to the region of a cold target ahead of the thermal wave front, where they either produce bremsstrahlung in collisions with ions or generate line radiation, by knocking out electrons from the K-shell of atoms [39–42]. We calculated the integrated intensity of hard X-rays under conditions close to our experiments. Because the intensity of light exceeded 10^{18} W cm^{-2}, the velocity of a fast electron was proportional to c. In this case, the dependence of bremsstrahlung of the electron distribution function calculated with the help of the KINET code is logarithmic, and the total power emitted by unit volume of the plasma is of the order of $(Ze^6 n_e/m^2c^4)\ln(\pi m v_E^2/h w_X)$ [47].

The duration of the X-ray pulse (~ 0.1 ps) is determined by the lifetime of the fast electron $\tau_e \approx 1/n_i v_h \sigma_{in}$, where σ_{in} is the cross section for inelastic scattering in the medium. The total energy of the pulse is $\varepsilon_X \approx e^6 Z n_e^2 l_s S\tau/hmc^2$, where S is the focal spot area. The coefficient of conversion k_{hX} of laser radiation to hard X-rays calculated with the help of the KINET code is shown in Fig. 5 [61]. Its behavior agrees with experimental results [43–46], and it is equal to 10^{-4} under our conditions.

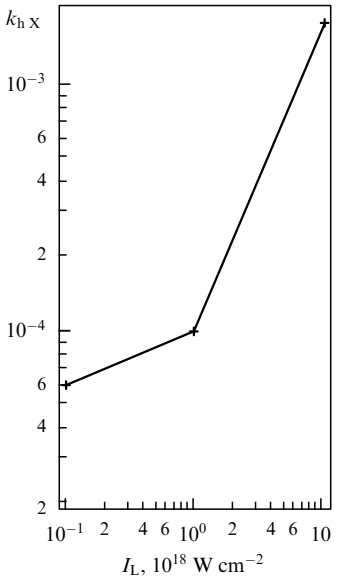

Figure 5. The coefficient of conversion of laser radiation to hard X-ray as a function of the laser generation efficiency.

Within 0.1 ps of the termination of the laser pulse the X-ray radiation does not completely vanish but is replaced by soft X-rays. Note that because fast electrons have relativistic velocities, the generation of hard X-rays will occur in the direction of the movement within the narrow angle $\Delta\theta \sim 1/\gamma$, where γ is the relativistic factor.

3.4 Generation of fast particles

The flux of fast ions was first observed in experiments with a picosecond plasma [12, 50]. For $I_L \approx 10^{17}$ W cm^{-2}, fast electrons appearing due to resonance absorption will disperse to vacuum and accelerate ions due to the ambipolar

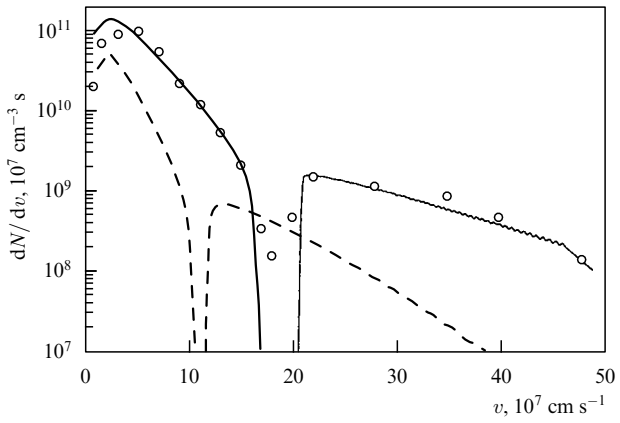

Figure 6. Spectrum of ion velocities upon the interaction of the P-polarized 1.5-ps Gaussian pulse from a Nd:glass laser incident on an aluminium target at an angle of 45° for a pulse intensity $I = 10^{16}$ W cm^{-2} (dashed curves) and 10^{17} W cm^{-2} (solid curves). The experimental points correspond to an intensity of 10^{17} W cm^{-2}.

field [35]. SKIN calculations of parameters of fast ions for laser pulses used in our experiments are presented in Fig. 6. The energy of the fast ions can be estimated from the temperature of fast electrons: $E_{hi} \sim Mc_s^2 \sim T_h \sim 1$ MeV, in accordance with the experiment [59]. The coefficient of conversion to megaelectronvolt ions increases with increasing laser intensity as I^2. Note that even in the case of a laser intensity of 5×10^{17} W cm^{-2}, the density profile becomes steeper and the critical surface moves inside the target, which was observed from the red shift of radiation at 2ω in experiments [51, 52].

Of interest is the movement of electrons and ions in vacuum caused by the laser field. Thus, in Ref. [54] a flux of fast electrons was detected which moved in the direction of the reflected laser beam, whereas ions moved normally to the target [59, 60]. In [53, 55], the diagram of escape of fast electrons and ions was calculated with the help of 2D PIC code, which is qualitative agreement with experimental results.

For relativistic intensities, we can determine the velocity of ions moving inside the target as [25]

$$u = c\left[\frac{Z}{A}\frac{m_e}{m_p}\frac{n_c}{n_e}\left(\frac{I\lambda^2}{2.7\times 10^{18}}\right)\right]^{1/2}.$$

If these ions are tritons and the target consists of tritium on a lithium substrate, a thermonuclear reaction is possible [57] with the neutron yield:

$$N_n \sim N_t \sigma^{(t+Li)} n_{nu}^{Li} l_{eff}^{i} \sim 10^{-2} N_{he}.$$

Here, N_t is the total number of fast ions with the energy $\varepsilon = Mu^2/2$,

$$l_{eff}^{i} = \frac{\varepsilon^2}{2\pi} Z^{Li} n_{nu}^{Li} e^4 \ln\left(4\frac{\varepsilon}{I_i}\right);$$

is their range, and N_{he} is the number of fast electrons. In experiments [58] with a laser radiation intensity of $I = 10^{18}$ W cm^{-2}, a neutron yield $N_n \sim 200$ was detected.

One can see from the diagram that intense laser pulses can be also used for generation of positrons. Analysis of cross

sections for different reactions under our conditions shows that in materials with high values of Z, the channel dominates which is related to the conversion of a γ-quantum in the nuclear field to the electron-positron pair. In a gold target, this channel produces an order of magnitude more pairs than the channel of electron – ion collisions [57]. Thus, with the help of laser pulses of intensity 10^{21} W cm^{-2}, a source of positrons can be obtained which produces 10^{12} particles during the laser pulse. It was shown in Ref. [49] that due to the spatial separation of charges, a narrow positron flux can be obtained from a foil target.

4. Conclusions

(1) Laser systems have been devised capable of focusing 1-ps radiation pulses onto a target to achieve a power density of 10^{19} W cm^{-2}.

(2) A number of diagnostics have been developed for measuring the parameters of a laser plasma, as well as the computer codes PIKA, SKIN, ION, and KINET for the numerical simulation of laser-plasma systems.

(3) It has been shown that absorption of laser radiation obliquely incident on a flat target decreases with increasing intensity and the absorption coefficient reaches 30% for a power density of 10^{19} W cm^{-2}, while the difference in absorption of S- and P-polarized radiation decreases with increasing laser radiation intensity.

(4) It was shown that the intensity of X-ray radiation lines can be substantially increased using time profiling of the laser pulses. A conversion coefficient to the He$-\alpha$ line of $k_X \approx 0.5\%$ was obtained. A source of X-rays with an intensity up to 10^{15} W cm^{-2} has been developed.

(5) It was found that fast particles leave the target surface in an anisotropic way, electrons moving near the direction of the reflected light pulse and ions moving along the normal to the target surface. Megaelectronvolt ions and electrons with energies above 10 MeV were detected.

(6) The yield of positrons and neutrons produced by irradiation of a solid target by relativistic laser pulses was calculated. It was shown that approximately 10^7 positrons can be produced per laser pulse.

Acknowledgements. This work was supported by the International Scientific and Technological Center.

References

1. Afanas'ev Yu V et al. *Trudy FIAN* **134** 3, 32, 42, 52, 98, 100, 103, 167 (1982)
2. Perry M D, Mourou G *Science* **264** 917 (1994)
3. Pukhov A, in *Technical Program IX Conference on Laser Optics* (St. Petersburg, June 22 – 26, 1998) p. 49
4. Andreev A A, Mak A A, Yashin V E *Kvantovaya Elektron.* (Moscow) **24** 99 (1997) [*Quantum Electron.* **27** 95 (1997)]
5. Van'kov A B et al *Opt. Spektrosk.* **84** 94 (1998)
6. Borodin V G et al. *Kvantovaya Elektron.* (Moscow) **25** 115 (1998)
7. Alekseev V N et al. *Izv. Akad. Nauk SSSR, Ser. Fiz.* **48** 1477 (1984)
8. Chernov V N et al., in *Superstrong Fields in Plasmas* (AIP Conf. Proc., Vol. 426, Eds M Lontano et al.) (New York: AIP, 1998) p. 450
9. Malinov V A et al., in *Superstrong Fields in Plasmas* (AIP Conf. Proc., Vol. 426, Eds M Lontano et al.) (New York: AIP, 1998) p. 439
10. Borodin V G et al., in *Superstrong Fields in Plasmas* (AIP Conf. Proc., Vol. 426, Eds M Lontano et al.) (New York: AIP, 1998) p. 445
11. Kieffer J C et al. *Phys. Rev. Lett.* **62** 760 (1989)
12. Meyerhofer D D et al. *Phys. Fluids B* **5** 2584 (1993)
13. Sauerbrey R et al. *Phys. Plasmas* **1** 1635 (1994)
14. Rozmus W, Tikhonchuk V T *Phys. Rev. A* **42** 7401 (1990)
15. Pert G J *Phys. Rev. E* **51** 4778 (1995)
16. Andreev A A et al., in *Laser Optics'95 and ICONO'95* (Pros. SPIE, Vol. 2770, Eds A A Andreev, V M Gordienko) (Bellingham, WA: SPIE, 1996)
17. Ginzburg V L *Rasprostranenie Elektromagnitnykh Voln v Plazme* (The Propagation of Electromagnetic Waves in Plasmas) (Moscow: Fizmatlit, 1960) [Translated into English (International Series of Monographs on Electromagnetic Waves, Vol. 7) (Oxford: Pergamon Press, 1964)]
18. Kruer W L *The Physics of Laser Plasma Interactions* (Frontiers in Physics, Vol. 73) (Redwood City, Calif.: Addison-Wesley, 1988)
19. Andreev A A, Semakhin A N, in *Laser Applications* (Proc. SPIE, Vol. 2097, Ed. A A Mak) (Bellingham, WA: SPIE, 1993) p. 326
20. Brunel F *Phys. Rev. Lett.* **59** 52 (1987)
21. Andreev A A et al. *Zh. Eksp. Teor. Fiz.* **101** 1808 (1992) [Sov. Phys. JETP **74** 963 (1992)]; Andreev A A, Platonov K Yu *Fiz. Plazmy* **24** 26 (1998)
22. Gibbon P, Foerster E *Plasma Phys. Control. Fusion* **38** 769 (1996)
23. Gibbon P *Phys. Rev. Lett.* **76** 50 (1996)
24. Andreev A A, Platonov K Yu, Tanaka K, in *Proc. JAERI-Conf. 98-004* (March 1998) p. 37
25. Wilks S C et al. *Phys. Rev. Lett.* **69** 1383 (1992)
26. Estabrook K et al. *Phys. Rev. Lett.* **50** 2082 (1983)
27. Stamper J A et al. *Phys. Rev. Lett.* **26** 1012 (1971)
28. Sudan R N *Phys. Rev. Lett.* **70** 3075 (1993)
29. Ruhl H, Mulser P *Phys. Lett. A* **205** 388 (1995)
30. Askar'yan G A et al. *Fiz. Plazmy* **21** 884 (1995) [*Plasma Phys. Rep.* **21** 835 (1995)]
31. Andreev A A et al. *Kvantovaya Elektron.* (Moscow) **23** 907 (1996) [*Quantum Electron.* **26** 884 (1996)]
32. Limpouch J, Andreev A A, Semakhin A N *Iodine Lasers and Applications* (Proc. SPIE, Vol. 1980, Eds M Chirejka, J Kodymova) (Bellingham, WA: SPIE,1993)
33. Rae S C, Burnett K *Phys. Rev. A* **44** 3835 (1991)
34. Davis J, Clark R, Guiliani J *Laser Particle Beams* **13** 3 (1995)
35. Gurevich A V, Meshcherkin A P *Zh. Eksp. Teor. Fiz.* **80** 1810 (1981) [*Sov. Phys. JETP* **53** 937 (1981)]
36. Bell A R et al. *Plasma Phys. Control. Fusion* **39** 653 (1997)
37. Andreev A A, Kurnin I V *J. Opt. Soc. Am. B* **13** 2 (1996)
38. Andreev A A et al. *Kvantovaya Elektron.* (Moscow) **24** 79 (1997) [*Quantum Electron.* **27** 76 (1997)]
39. Audebert P et al. *Europhys. Lett.* **19** 189 (1992)
40. Chen H et al. *Phys. Rev. Lett.* **70** 3431 (1993)
41. Rousse A et al. *Phys. Rev. E* **50** 2200 (1994)
42. Schnurer M et al. *Phys. Plasmas* **2** 3106 (1995)
43. Kmetec J D et al. *Phys. Rev. Lett.* **68** 1527 (1992)
44. Soom B et al. *J. Appl. Phys.* **74** 5372 (1993)
45. Jiang Z et al. *Phys. Plasmas* **2** 1702 (1995)
46. Hares J D et al. *Phys. Rev. Lett.* **42** 1216 (1979)
47. Andreev A A et al. *Laser Optics'95 and ICONO'95* (Proc. SPIE, Vol. 2770, Eds A A Andreev, V M Gordienko) (Bellingham, WA: SPIE, 1996)
48. Ruhl H *Phys. Plasmas* **3** 3129 (1996)
49. Lykov V A, Gryznykh D A, Kandiev Ya Z *Report at 13 LIRPP* (13 – 18 April, Monterey, USA) Book of abstracts
50. Fews A P et al. *Phys. Rev. Lett.* **73** 1801 (1994)
51. Andreev A A et al., in *Superstrong Fields in Plasmas* (AIP Conf. Proc., Vol. 426, Eds M Lontano et al.) (New York: AIP, 1998) p. 61
52. Kalashnikov M P et al. *Phys. Rev. Lett.* **73** 260 (1994)
53. Estabrook K G, Valeo E J, Kruer W L *Phys. Fluids* **18** 1151 (1975)
54. Gauthier J-C J et al., in *Application of X Rays Generated from Lasers and Other Bright Sources (*Proc. SPIE, Vol. 3157, Eds G A Kyrala, J C J Gauthier) (Bellingham, WA: SPIE, 1997)
55. Litvinenko I A, Andreev A A, Platonov K Yu, in *Technical Program IX Conf. on Laser Optics* (St. Petersburg, 22 – 26 June, 1998) p. 62
56. Denavit J *Phys. Rev. Lett.* **69** 3052 (1992)
57. Andreev A A, Platonov K Yu, in *Technical Digest, Int. Conf. on LASERS' 97* (15 – 19 December 1997, The Fairmont Hotel, New Orlean, Louisiana) p. 29
58. Pretzler G et al., in *Technical Digest, Int. Conf. on LASERS' 97* (15 – 19 December 1997, The Fairmont Hotel, New Orlean, Louisiana) p. 22
59. Andreev A A et al., in *Technical Program IX Conf. on Laser Optics* (St. Petersburg, 22 – 26 June, 1998) p. 49

60. Komarov V M et al., in *Technical Program IX Conf. on Laser Optics* (St. Petersburg, 22 – 26 June, 1998) p. 61
61. Andreev A A, Platonov K Yu, Gauthier J - C, in *Technical Digest, Application of High Field and Short Wavelength Sources VII* (19 – 22 March, 1997) p. 20

PACS number: 42.62.Hk

Femtosecond plasma in dense nanostructured targets: new approaches and prospects

V M Gordienko, A B Savel'ev

1. Introduction

The recent advent of a new generation of terawatt femtosecond laser systems (FLS) (1 TW = 10^{12} W, 1 fs = 10^{-15} s) opens up fundamentally new possibilities for studying the interaction of radiation with matter and numerous applications in various fields of science and engineering. FLSs provide terawatt powers even at quite low light pulse energies from 10 to 100 mJ and the 10 – 100-fs pulse duration, which allows one, by focusing laser radiation, to obtain a huge power density light field exceeding 10^{16} W cm^{-2} (of the order of the Coulomb field in a hydrogen atom). Such superintense laser radiation, which cannot be obtained by any other method under laboratory conditions, permits the study of fundamental properties of matter under extreme conditions.

The development of this new tool for studies has a revolutionary significance for science, which can be compared with the creation of energy sources based on nuclear reactions. However, note here the fundamental difference related, first, to the miniaturization of the region of energy concentration (about 10^{-11} cm^3), which excludes the influence of the social factor on these studies despite the huge energy flux of the order of 10^{11} J cm^{-3}, and second, to the comparatively low-cost experimental setups. The advent of new types of FLSs has stimulated studies of the behavior of substances under conditions far from equilibrium. Such a statement of the problem is typical not only for fundamental studies in the fields of physics, chemistry, and biology, but also for applied studies devoted to the development of new promising technologies, which is reflected in an avalanche-like increase in the number of papers in this field and in the use of FLSs in main universities and scientific laboratories abroad. FLSs of the new generation have become basic instruments for multidisciplinary investigations.

The use of ultrashort light pulses fundamentally changes the process of interaction of laser radiation with matter, because the energy is absorbed in a thin solid layer before its hydrodynamic expansion to vacuum takes place. For femtosecond laser radiation intensities above 10^{15} W cm^{-2}, electrons acquire an energy of hundreds and thousands of electronvolts during the laser pulse, independent of the target material, resulting in the formation of a femtosecond laser plasma (FLP). The ion temperature does not vary noticeably, and after termination of the laser pulse, a strongly nonequilibrium plasma is produced in the interaction region, in which the electron subsystem has an energy that is, on the one hand, sufficient for generation of intense ultrashort X-ray radiation, stimulation of laser-controlled nuclear processes, etc. [1 – 3], and on the other hand, for efficient and precision evaporation of the irradiated volume, which forms the basis for the new femtotechnology of material processing [4 – 6].

In this paper, we report the main results obtained in the Laboratory of Superstrong Light Fields of the International Laser Center, M V Lomonosov Moscow State University, during recent years. The aim of our work is to study the ways for controlling processes proceeding in the FLP. We have shown that, by controlling plasma processes, we can produce FLP with the required temperature and electron and ion densities, and X-ray spectrum, or obtain a plasma with new combinations of these basic parameters.

A promising method for increasing absorption and 'effective' nonlinear optical susceptibility of the FLP is the excitation of surface electromagnetic waves (SEW) on targets with a periodical surface relief considered in the second section of this paper. The third section is devoted to our experiments with FLP in ultrathin freely suspended carbon films, when the thermal flow inside the target proves to be suppressed, resulting in FLP overheating. In the fourth section, we present studies of the formation and properties of a plasma in porous nanostructured substances.

Experiments were performed using the femtosecond excimer laser system, which produced a superstrong light field and has been described in a number of papers [6 – 9]. We devised a diagnostic system for studies of the FLP in our laboratory, which provided the following measurements: control of the accuracy of focusing to a spot of diameter 3 μm with the help of the second-harmonic signal in reflection and by measuring the total energy of X-ray radiation from the plasma in the energy range $E > 3$ keV using a photomultiplier with a NaJ(Tl) scintillator; detection in the second identical channel equipped with changeable filters of quanta with energies $E > 5 – 50$ keV; and detection of soft X-ray radiation by p-i-n diodes with filters ($0.05 < E < 1$ keV). The velocity of plasma expansion was measured with a time-of-flight detector based on an electron multiplier equipped with a microchannel plate.

2. Excitation of surface electromagnetic waves

Because the modulus of the wave vector of the SEW in the FLP exceeds that of the wave vector of the incident radiation, we compensated for this mismatching by using a periodically modulated surface [9 – 11]. We demonstrated for the first time the resonance generation of the second harmonic upon excitation of the SEW in the FLP and showed that SEWs modify parameters of the FLP by increasing the local-field effect, and the process of the second-harmonic generation is a sensitive indicator of the SEW excitation.

3. 'Overheating' of the femtosecond laser plasma in freely suspended thin-film targets

We carried out a series of studies [9, 12 – 14] devoted to the efficient generation of X-rays in the region of the water window[1] upon irradiation of freely suspended carbon films by femtosecond pulses of 10^{15} W cm^{-2} intensity. We showed that the optimum thickness of the film was 20 – 30 nm. For a thinner film, the conversion efficiency decreases due to the rapid hydrodynamic disintegration of the film over a time shorter than the laser pulse duration. These experimental data were confirmed by a numerical experiment, which showed

[1] The water window is the transparency region of water between 2.3 and 4.4 nm, which is optimal for microscopy of biological objects.